Bull. Natl. Mus. Nat. Sci., Ser. C, 49, pp. 1–13, December 20, 2023

DOI: 10.50826/bnmnsgeopaleo.49.0_1

Albian (Early Cretaceous) U-Pb age of detrital zircons for a coal-associated sandstone (Lipovtsy Formation, Nikan Group) in SW Primorye, Russia: Paleofloristic and provenance comparison with the Tetori Group in the Hida belt, Japan

Yukio Isozaki[1, *], Yukiyasu Tsutsumi[2], Tomohito Nakano[1], Victor Nechaev[3], Yuri Zakharov[3] and Alexander Popov[3]

[1] Department of Earth Science and Astronomy, The University of Tokyo, Komaba, Meguro, Tokyo 153–8902, Japan

[2] Department of Geology and Paleontology, National Museum of Nature and Science, Amakubo, Tsukuba 028–0005, Japan

[3] Far East Geological Institute, Far Eastern Branch, Russian Academy of Sciences, Vladivostok 690022, Russia

[*]Author for correspondence: isozaki@ea.c.u-tokyo.ac.jp

Abstract U-Pb ages of detrital zircons were measured by LA-ICPMS for a Lower Cretaceous coal-associated sandstone in the Laoelin-Grodekov (L-G) belt, South Primorye, Russia. The non-marine Lipovtsy Formation in the Razdolʹnaya coal basin is enriched in coal seams and Early Cretaceous paleoflora called the "Late Lipovtsy floristic assemblage", which is characterized by diverse ferns, gymnosperms, and the earliest angiosperms. Dated zircons from the Upper Lipovtsy Fm contain abundant Jurassic grains with the youngest of 112 Ma (early Albian). The estimated depositional age of the sandstone, the early Albian or younger, constrains the appearance timing of angiosperms in Primorye to be no earlier than the Albian, slightly younger than previously thought. The age spectrum of detrital zircons of the upper Lipovtsy sandstone is characterized by the abundance in Early Jurassic grains with minor amount of Triassic and Early Cretaceous ones and without Precambrian ones. This pattern is nearly identical to those of coeval sandstones deposited on the Jiamusi block (Greater South China: GSC; China/Russia), Central Asian orogenic belt (China/Mongolia), and the Hida belt (Japan). These similarities in detrital zircon ages and paleofloras support the pre-Japan Sea connection between the L-G and Hida belts developed on the west of GSC.

Key words: non-marine Cretaceous, Laoelin-Grodekov belt, flora, Greater South China, Hida belt

Introduction

The major distribution of Cretaceous System in Far East Asia, mostly non-marine in nature, is known from the Songliao basin in NE China and the Dasanjiang basin around China/Russia border, with their satellite basins around the Russia/China/North Korea borders (Fig. 1; e.g. Kirillova, 2018; Kosenko *et al.*, 2021). These strata were deposited unconformably on the Jurassic and older basement rocks of the eastern segment of the Central Asian orogenic belt (CAOB) and of the Greater South China block (GSC; Isozaki *et al.*, 2014, Isozaki, 2019), which was formed through the convergent assembly of major continental blocks, i.e., Siberia, North China, and GSC, during the Late Paleozoic-Early Mesozoic.

Mostly in the drainage of the Razdolʹnaya River in SW Primorye, Far East Russia, there is a domain of thick Cretaceous marine/non-marine strata in the Laoelin-Grodekov (L-G) belt on the east of CAOB (Fig. 1B), which represents one of the satellite basins of the main Songliao basin. Because of the extensive occurrence of coal-bearing Cretaceous terrigenous clastic strata, this domain is called the Razdolʹnaya coal basin (Kovaleva *et al.*, 2016; Volynets and Bugdaeva, 2017; Kosenko, 2021). The coal-bearing non-marine beds yield well-preserved plant fossils composed mostly of warm climate-adapted ferns and gymnosperms (Volynets and Bugdaeva, 2017; Kirillova, 2018). This paleoflora shows a remarkable contrast with the coeval cooler

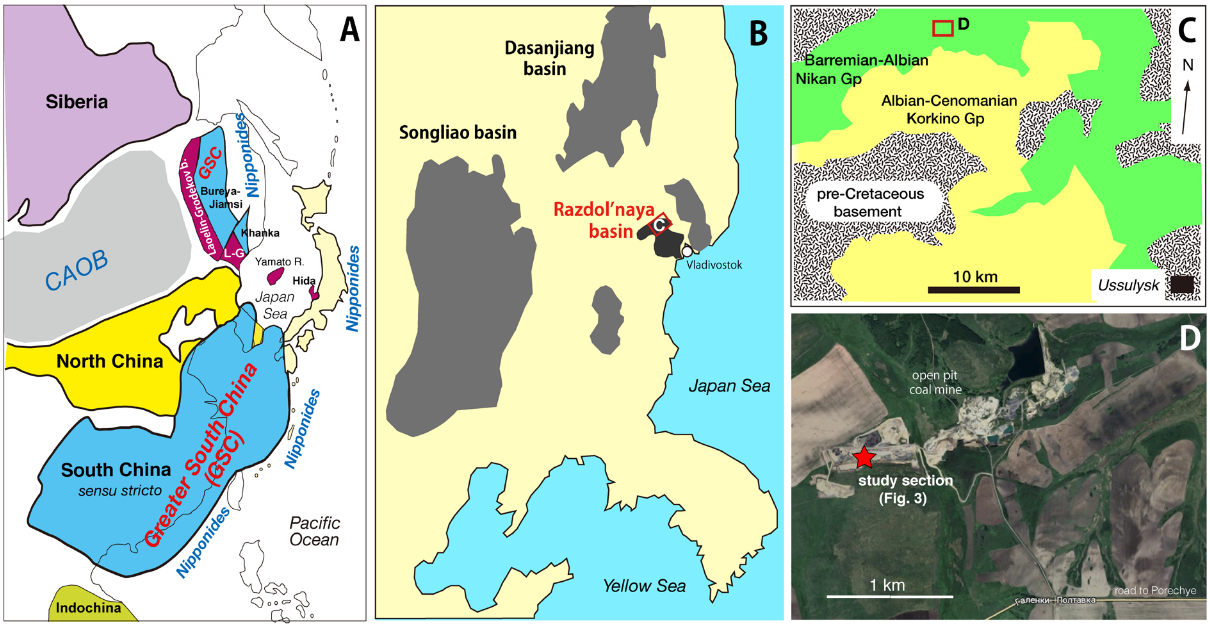

Fig. 1. Index geotectonic map of Far East Asia (A; modified from Isozaki, 2019), index map of major Cretaceous basins (gray) with the Razdol'naya coal basin (dark gray) in South Primorye, Russia (B; simplified from Kirillova, 2018), local geologic map of the northern Razdol'naya basin (C; simplified from Volynets and Bugdaeva, 2017) with the location of study section (red square), and a satellite image (Google Earth) of the study section in the open-pit coal mine near Porechye (D).
Note that the Laoelin-Grodekov belt in Far East Asia, including the Hida belt, represents a major tectonic element that divide the CAOB and the Pacific rim geotectonic units, i.e., Greater South China and Nipponides (Isozaki, 2019).

climate-adapted paleoflora in Siberia on the north. The depositional age of the main coal bed was dated Aptian (early Cretaceous) by U-Pb age of zircons from a tuff bed (Volynets and Malinovsky, 2020).

It is noteworthy that a nearly identical Cretaceous flora is known in Japan; i.e. the Tetori flora from the non-marine Tetori Group particularly in the Hida belt, Japan (Kimura, 1979). In addition, the rest of the Japanese archipelagos and Sakhalin Island along the Pacific margin have a distribution of Lower Cretaceous System of shallow marine facies (e.g. Tanaka, 1977; Ando and Takahashi, 2017), which were deposited, in contrast, on the Nipponides orogenic belt (Sengör and Natal'in, 1996) along the Pacific side of GSC for over 2500 km (Isozaki, 2019; Hasegawa *et al.*, 2020) and with the warmer climate-adapted Ryoseki flora (Kimura, 1979). Nonetheless, the mutual correlation among these has been still unsatisfactory with poor age constraints. For reconstructing pre-Japan Sea paleogeographic framework of Far East Asia, provenance analysis for clastic rocks is inevitable.

For obtaining age and provenance information, this study analyzed U-Pb ages by LA-ICPMS of detrital zircon from the non-marine Cretaceous strata in the Razdol'naya coal basin in southern Primorye. This short article reports new zircon U-Pb ages and discusses their implication to the provenance of the mid-Cretaceous basins in southern Primorye with respect to that of the coeval Tetori Group in Japan.

Geologic Setting

The pre-Cenozoic geotectonic framework of Far East Asia is recently drawing much attention due to the emerging geological significance of CAOB, although the study on the peri-Japan Sea region around the borders among Russia, China, and N. Korea has been delayed with respect to the rest of Far East Asia. Three major Precambrian blocks forming Far East Asia are Siberia, North China, and GSC (Fig. 1A; e.g. Maruyama *et al.*, 1989; Jahn, 2004; Domier *et al.*, 2018; Isozaki, 2019), which were primarily derived from the breakup of the Neoproterozoic supercontinent Rodinia (e.g. Hoffman, 1991) and merged again during the Late Paleozoic-Triassic interval by the closure of a vast oceanic domain called the Paleo-Asian Ocean. CAOB is the total consequence of such multiple plate convergence in this past ocean.

The geotectonic framework of southern Primorye is largely characterized by the N-S trending structures of multiple geotectonic units (e.g. Melʹnikov and Izosov, 1984; Zakharov *et al.*, 1992; Khanchuk *et al.*, 1996; Fig. 1A). The unit around the Khanka Lake on the border between NE China and Primorye is traditionally called the Khanka block (Fig. 1A), which was lately regarded as a northern segment of GSC, as well as the north-neighboring Jiamusi and Bureya blocks in China and Primorye (Isozaki *et al.*, 2017; Isozaki, 2019). On the eastern side of GSC, plural belts of subduction-related origin occur, i.e., the Sergeevka, Samarka, Zuravlevka, and Taukha belts (e.g. Khanchuk *et al.*, 1996; Kojima *et al.*, 2000; Kemkin, 2012; Fig. 1A). Like the correlative units in Japan, they totally belong to the Phanerozoic subduction-related Nipponides orogenic belt (Sengör and Natalʹin, 1996), which developed along a long-lasting trench on the Pacific side of GSC (Isozaki *et al.*, 2014, 2017; Isozaki, 2019) before the Miocene opening of the Sea of Japan (e.g. Otofuji *et al.*, 1981; Tamaki, 1988).

On the other hand, the neighboring unit on the west/southwest of the Khanka block (= GSC) is the L-G belt along the Japan Sea coast, of which width is over 100 km in E–W direction over the Russia/China/N. Korea borders (Fig. 1). Together with its possible extension into the Yamato Ridge in the mid-Japan Sea and the Hida belt in central Japan (Fig. 1A), the L-G belt represents the easternmost remnant of the closed Paleo-Asian Ocean among the Siberia, GSC and N. China blocks (Isozaki *et al.*, 2023).

The study area in the Razdolʹnaya basin with the non-marine Cretaceous strata is located in the southern half of the L-G belt in SW Primorye, clearly separated from the major Cretaceous basin of Songliao on the west (Fig. 1B). The Lower Cretaceous strata of the Razdolʹnaya basin are called Nikan Group, which comprise terrigenous clastic rocks of the following three formations; i.e., the Ussuri Fm, Lipovtsy Fm, and Galenka Fm, in ascending order (Krassilov, 1967; Fig. 2). On the basis of lithological and paleofloristic correlation, this group is assigned to the Barremian to Albian (Lower Cretaceous) (Golozoubov *et al.*, 1999; Kovaleva *et al.*, 2016; Kirillova, 2018; Kosenko *et al.*, 2021).

The Lipovtsy Fm, ca. 500 m thick, is composed of sandstone and mudstone with multiple coal seams, which represent a marsh facies. A tuff bed in the major coal seam was recently dated by zircon U-Pb age of 117 Ma (Aptian) (Volynets and Malinovsky, 2020; Fig. 2). This formation yields abundant plant fossils, such as tree trunks, leaves, and spores/pollens (Golozoubov *et al.*, 1999; Kovaleva *et al.*, 2016; Volynets and Bugdaeva, 2017; Kirillova, 2018). The upper half of the Lipovtsy Fm contains a prominent coal seam of up to 19 m thick (Fig. 2 showing its topmost 7 m-thick interval). The overlying sandstones and coaly shales above this main coal seam yield well-preserved plant fossils, which is composed of 136 taxa, i.e., dominant and diverse ferns (*Nathorstia*, *Alsophilites*, *Onychiopsis* etc.), associated conifers (*Araucariodendron*, *Podozamites*, *Elatides*, *Torreya*, *Mirovia* etc.), and other gymnosperms (Benettitales, Cycadales, Lycopodiales, Ginkgoales, Czekanowskiales, and Gnetales). This fossil plant assemblage called the Late Lipovtsy floristic assemblage (FA) is unique in the association of ferns (*Nathorstia*), *Cycadites and Dictyozamites* (Benettitales), and *Torreya* (conifer), particulalrly with the most advanced ferns (*Osmunda* and *Birisia*) and the earliest angiosperms. This floral composition is distinct from those from the underlying beds of the group.

By comparing the paleofloras reported from Japan (Kimura, 1979), Golozoubov *et al.* (1999) correlated this floristic assemblage with the Tetori flora adapted to cooler-climate in Japan, rather than the Ryoseki-flora adapted to warm-climate from the rest of Japan; nonetheless, Ohana & Kimura (1995) mentioned that the Lipovtsy flora may represent a mixed flora between the typical two in Japan.

What is the most noteworthy is the earliest occurrence of some leaf (*Dictyophyllum*, *Onoana*) and pollen (*Tricolpites*) fossils of angiosperms from Primorye, although they are extremely rare. As their occurrence is none in the main coal seam but solely from the overlying clastic beds in the section (Fig. 2; Kovaleva *et al.*, 2016), precise dating for their first appearance timing is critical and required for evaluating the significance.

Sample and Analytical

Sample: The analyzed sample PR6 was collected at the new open-pit coal mine located ca. 3 km to the west of Porechye village (44°7′50″N, 131°49′15″E; Fig. 3). The outcrop shown in Fig. 3B

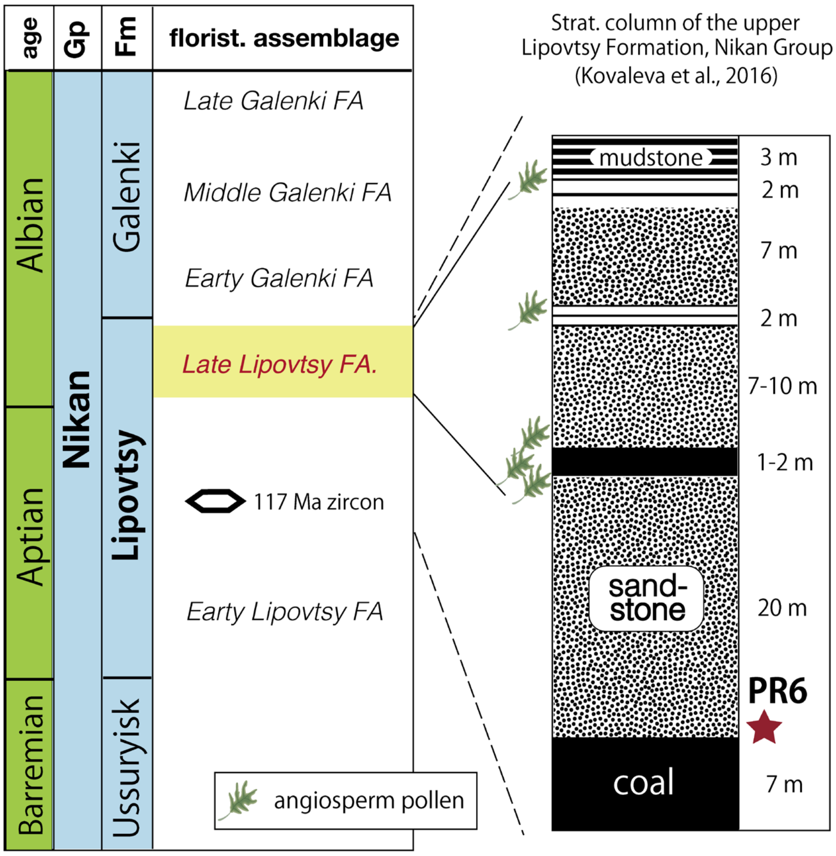

Fig. 2. Correlation diagram of the Nikan Group in southern Primorye (left: Kosenko *et al.*, 2021) and the stratigraphic column of the study section at the Porechye open-pit coal mine near the study section (right: Kovaleva *et al.*, 2016) with the sample horizon (red star).
Note that the first appearance horizon of angiosperm (pollen) in the Upper Lipovtsy Fm is nearly 20 m above the horizons of dated sample PR6.

Fig. 3. Outcrop views of the study section at an open-pit coal mine with the main coal seam and overlying sandstone of the upper part of the Lipovtsy Formation (photos taken on Sept. 8, 2019).
The sharp lithologic change from the main coal seam (below) to thick sandstone (above) (Fig. 2) suggests a possible hiatus between them with a potential age gap. Angiosperm pollens occur solely from the sandstone and above, whereas none from the main coal seam dated as the Aptian.

exposes the basal part of the upper half of the Lipovtsy Fm. The sample PR6 is a yellowish light grey, medium-grained sandstone, of which stratigraphic horizon is immediately above the main coal seam (Figs. 2, 3).

Analytical: Zircon grains were handpicked from heavy fractions that were separated from the rock samples by standard crushing and heavy-liquid techniques at Department of Earth Science and Astronomy, The University of Tokyo. The separated zircon grains, zircon standards FC1 (1099 Ma; Paces and Miller, 1993) and OD3 (33 Ma; Iwano *et al.*, 2013), and the glass standard NIST SRM610 were mounted in an epoxy resin and polished till the center of the embedded grains exposed in the surface. After polishing, backscattered electron (BSE) and cathodoluminescence (CL) images of the mounted zircons were checked for selecting sites for analysis. For BSE and CL images, a scanning electron microscope-cathodoluminescence equipment, JSM-6610 (JEOL) and a CL detector (Sanyu Electron), were used. U-Pb dating of these samples was carried out using an LA-ICP-MS which constitutes a NWR213 (Elemental Scientific Lasers) and Agilent 7700x (Agilent Technologies) at the National Museum of Nature and Science, Tsukuba, Japan. The experimental conditions and analytical procedures were according to Tsutsumi *et al.* (2012), and additional devices of a buffered type stabilizer (Tunheng and Hirata, 2004) were applied. The spot size of the laser was 25 µm. A correction for common Pb was made based on the measured ^{208}Pb/^{206}Pb and Th/U ratios (^{208}Pb correction) (e.g. Williams, 1998) and the model for common Pb compositions proposed by Stacey and Kramers (1975). Pb* indicates radiometric Pb. The criterion of concordant is for 2σ overlap of the concordia curve on a concordia diagram. ^{238}U-^{206}Pb* ages are used for less than 1000 Ma data and ^{207}Pb*/^{206}Pb* ages are used for the other data. The data of secondary standard OD3 zircon obtained during analysis yielded weighted mean ages of 31.3 ± 1.5 Ma (n = 6; MSWD = 0.76). MSWD is an acronym of mean square weighted deviation calculated from the square root of the χ^2 value.

Results

All of the hand-picked zircon grains have clear oscillatory zoned texture (Fig. 4A). We measured U-Pb ages for 82 euhedral zircon grains from sample PR6. Table 1 shows all measurements of analyzed zircons. All U-Pb ages of analyzed spots/grains were concordant (Fig. 4B). U-Pb ages of detrital zircons from Sample PR6 range from 417.6 ± 5.6 to 111.8 ± 2.0 Ma. For more than two thirds in number, Early Jurassic (ca. 200–180 Ma) grains dominate, whereas Triassic (220–200 Ma) and Early Cretaceous (140–110 Ma) ones are minor. No Precambrian zircon was detected.

The youngest single grain age (YSG) and weighted mean of youngest cluster of more than 2 grain ages that overlap in age within 1σ error (YC1σ) (Dickinson and Gehrels, 2009) are used to show older limit of deposition age. In principle, YSG should indicate the older limit of the depositional age, but estimation based on ages from multiple grain are generally more consistent (Dickinson and Gehrels, 2009). In this study, we treat the YC1σ ages as the older limit of depositional age. Three youngest grains are 111.8 ± 2.0, 112.1 ± 2.6 and 112.3 ± 2.6 Ma, and YC1σ is 112.7 ± 1.1 Ma (n = 5, MSWD = 0.19). These ages all correspond to the earliest Albian, Early Cretaceous (according to Cohen *et al.*, 2013; the same afterwards).

Discussion

Depositional age: On the basis of YC1σ at 112.7 ± 1.1 Ma, the depositional age of the sandstone (PR6) in the lower part of the Upper Lipovtsy Fm (Figs. 2, 3) is constrained to the early Albian or younger. This age assignment is concordant with the previous estimate, i.e., the Aptian-early Albian for the entire formation, which was based on the local stratigraphical correlation (Kovaleva *et al.*, 2016; Volynets and Bugdaeva, 2017) and zircon U-Pb age of a tuff bed within the main coal seam (Volynets and Malinovsky, 2020; Fig. 2).

The lithofacies change is remarkably sharp between the top of major coal seam (~117 Ma) and the overlying 112 Ma or younger sandstone (Figs. 2, 3). In addition, a slightly oblique contact between the coal seam and sandstone suggests a hiatus of

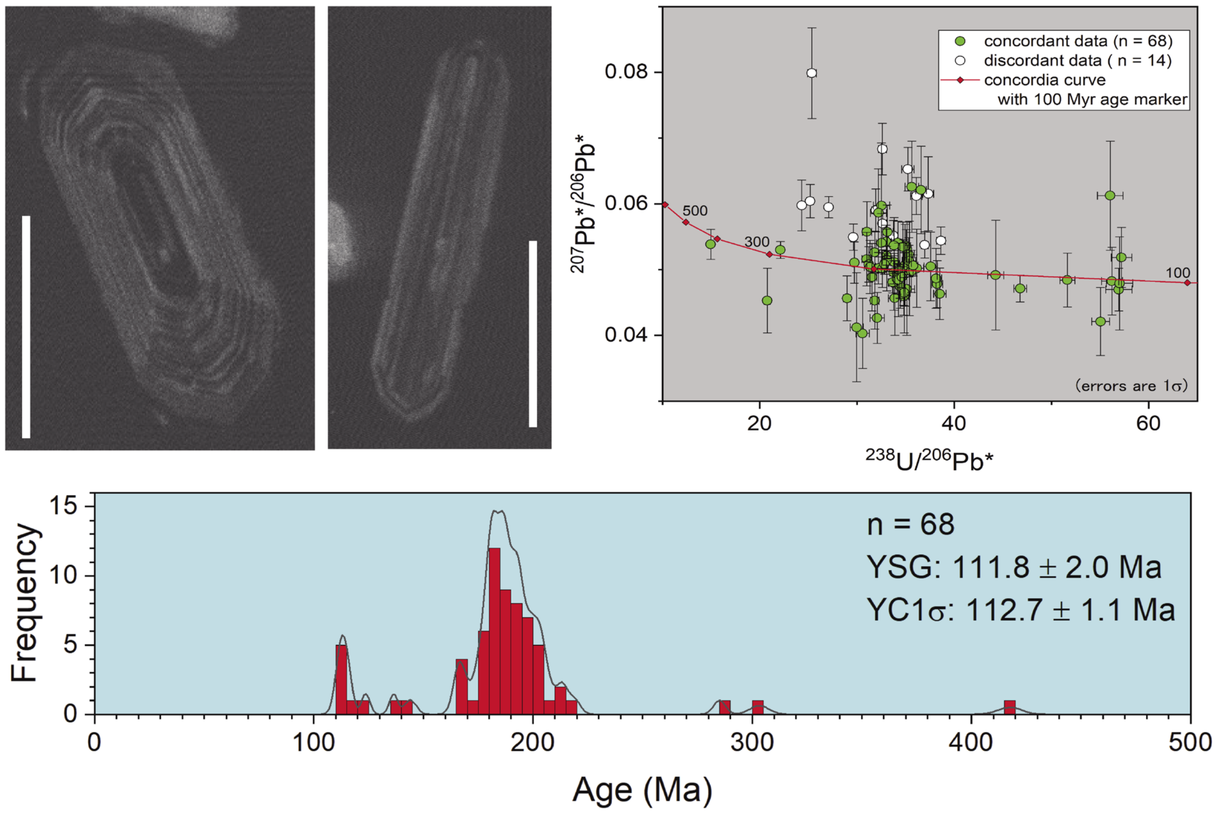

Fig. 4. Examples of cathode-luminescence image of dated zircons with scale bar of 100 micrometer (A), concordia diagram (B), and U-Pb age spectrum of detrital zircons in histogram and probability density curve (C) for analyzed sandstone (Sample PR6) from the Lipovtsy Fm, Nikan Group, in the Razdolʹnaya coal field, Primorye.

potential age gap between them. The depositional ages of the major coal seam and the underlying beds of the Lower Lipovtsy Fm likely remain within the Aptian, as previously suggested, whereas the overlying sandstones with the angiosperm-bearing Late Lipovtsy FA in the early Albian or younger age.

Emergence of angiosperm in Far East Asia: The uniqueness of the Late Lipovtsy FA is two-fold, i.e., in the mixed aspect of the cooler climate-adapted Tetori and warm climate-adapted Ryoseki floras, and in the association with the earliest angiosperms from Primorye. In a regional paleofloristic framework, Far East Asia is characterized by two provinces, i.e., the Siberian-Canadian realm and Euro-Sinian realm (Vakhrameev, 1978; Fig. 5) or the Tetori and Ryoseki floristic provinces with a transitional zone between the two (Kimura, 1979; Yabe *et al.*, 2003). The occurrence of the Late Lipovtsy FA marks the northernmost margin of the Euro-Sinian realm in Far East Asia during the Albian, immediately on the south of the southern Siberian-Canadian realm (Kilillova, 2018). The present age assignment is noteworthy for limiting the position of temperature/humidity-sensitive floristic province/realm boundary during the Albian, as to its possible northward shift under the claimed warming during the Early Cretaceous, of which aspect is much clearer with the appearance timing of angiosperms, as discussed below.

The world oldest angiosperm fossil was reported from the late Valanginian (Early Cretaceous) strata in Israel (Brenner, 1996), which were deposited in low-latitude northern Gondwana. Their distribution spread globally afterwards during the Barremian-Albian and became common in the whole world by the end-Cretaceous. In Far East Asia, the oldest occurrence of angiosperm (pollen) was reported from the Barremian Nishihiro Fm in the Pacific side of SW Japan (Legrand *et al.*, 2014), which is included in the warm climate-adapted Ryoseki flora. In the Aptian, they have appeared also in the cooler climate-adapted Tetori flora in the Japan Sea-side of SW Japan (Legrand *et al.*, 2019).

The present age confirmation of the first appearance timing of angiosperms in Primorye highlighted an apparent time lag with respect to those of the Japanese floras. As the first appearance of angiosperms in Primorye was no earlier than the early

Table 1. Measurements of U-Pb ages of zircons for Sample PR6 from the Lipovtsy Formation of the Nikan Group in southern Primorye, Russia.

Labels	$^{206}Pb_c$ (1) (%)	U (ppm)	Th (ppm)	Th/U	$^{238}U/^{206}Pb^*$ (1)	$^{207}Pb^*/^{206}Pb^*$ (1)	$^{238}U/^{206}Pb^*$ age (1) (Ma)	Remarks
PR6_001	0.17	135	88	0.67	35.10 ± 0.81	0.0470 ± 0.0070	181.1 ± 4.1	
PR6_002	0.83	375	187	0.51	30.99 ± 0.48	0.0516 ± 0.0041	204.7 ± 3.1	
PR6_003	0.74	893	332	0.38	32.21 ± 0.42	0.0502 ± 0.0024	197.1 ± 2.5	
PR6_004	0.15	526	160	0.31	34.19 ± 0.42	0.0541 ± 0.0033	185.8 ± 2.3	
PR6_005	0.00	303	166	0.56	25.18 ± 0.34	0.0604 ± 0.0025	251.1 ± 3.3	discordant
PR6_006	0.00	282	213	0.77	35.30 ± 0.57	0.0523 ± 0.0025	180.1 ± 2.9	
PR6_007	0.90	851	333	0.40	31.81 ± 0.37	0.0526 ± 0.0032	199.5 ± 2.3	
PR6_008	0.00	330	178	0.55	32.99 ± 0.53	0.0542 ± 0.0025	192.5 ± 3.1	
PR6_009	0.00	784	539	0.71	22.12 ± 0.22	0.0530 ± 0.0013	285.1 ± 2.8	
PR6_010	0.00	785	265	0.35	33.14 ± 0.40	0.0513 ± 0.0015	191.6 ± 2.3	
PR6_011	0.00	872	326	0.38	33.84 ± 0.37	0.0511 ± 0.0014	187.7 ± 2.0	
PR6_012	0.63	201	158	0.80	56.03 ± 1.32	0.0612 ± 0.0083	114.0 ± 2.7	
PR6_013	0.47	508	201	0.41	31.93 ± 0.43	0.0590 ± 0.0033	198.8 ± 2.6	discordant
PR6_014	4.73	803	435	0.56	35.12 ± 0.40	0.0532 ± 0.0040	181.0 ± 2.0	
PR6_015	0.93	188	63	0.35	34.78 ± 0.73	0.0496 ± 0.0050	182.8 ± 3.8	
PR6_016	0.00	765	373	0.50	38.62 ± 0.46	0.0544 ± 0.0021	164.8 ± 1.9	discordant
PR6_017	2.53	464	196	0.43	28.98 ± 0.38	0.0456 ± 0.0034	218.7 ± 2.8	
PR6_018	0.00	708	296	0.43	33.02 ± 0.41	0.0521 ± 0.0014	192.3 ± 2.4	
PR6_019	0.00	110	74	0.69	32.07 ± 0.73	0.0427 ± 0.0039	198.0 ± 4.5	
PR6_020	0.00	548	241	0.45	33.76 ± 0.42	0.0496 ± 0.0018	188.2 ± 2.3	
PR6_021	1.09	307	401	1.34	44.25 ± 0.83	0.0492 ± 0.0083	144.1 ± 2.7	
PR6_022	4.19	1603	667	0.43	35.05 ± 0.34	0.0536 ± 0.0025	181.3 ± 1.8	
PR6_023	4.78	1202	92	0.08	31.21 ± 0.33	0.0508 ± 0.0027	203.3 ± 2.1	
PR6_024	0.96	363	199	0.56	31.81 ± 0.45	0.0453 ± 0.0043	199.5 ± 2.8	
PR6_025	0.05	884	277	0.32	29.61 ± 0.35	0.0549 ± 0.0020	214.1 ± 2.5	discordant
PR6_026	1.04	397	301	0.78	35.38 ± 0.60	0.0502 ± 0.0072	179.7 ± 3.0	
PR6_027	1.12	482	278	0.59	31.02 ± 0.48	0.0557 ± 0.0046	204.5 ± 3.1	
PR6_028	0.06	481	340	0.72	37.31 ± 0.56	0.0615 ± 0.0056	170.5 ± 2.5	discordant
PR6_029	0.00	947	336	0.36	33.00 ± 0.37	0.0515 ± 0.0014	192.4 ± 2.1	
PR6_030	1.39	590	276	0.48	34.69 ± 0.46	0.0534 ± 0.0038	183.2 ± 2.4	
PR6_031	0.00	706	549	0.80	36.95 ± 0.37	0.0537 ± 0.0020	172.1 ± 1.7	discordant
PR6_032	2.18	693	560	0.83	36.58 ± 0.54	0.0621 ± 0.0066	173.8 ± 2.5	
PR6_033	3.46	534	206	0.40	38.24 ± 0.57	0.0478 ± 0.0036	166.4 ± 2.5	
PR6_034	1.22	182	87	0.49	34.92 ± 0.76	0.0507 ± 0.0062	182.0 ± 3.9	
PR6_035	0.80	174	85	0.50	36.14 ± 0.69	0.0502 ± 0.0060	175.9 ± 3.3	
PR6_036	0.59	565	449	0.81	34.40 ± 0.47	0.0499 ± 0.0042	184.7 ± 2.5	
PR6_037	0.89	391	227	0.60	56.21 ± 1.07	0.0483 ± 0.0052	113.7 ± 2.2	
PR6_038	2.85	680	307	0.46	32.61 ± 0.42	0.0683 ± 0.0039	194.7 ± 2.4	discordant
PR6_039	0.63	576	250	0.45	32.61 ± 0.43	0.0501 ± 0.0029	194.7 ± 2.5	
PR6_040	0.37	247	174	0.72	37.57 ± 0.68	0.0505 ± 0.0052	169.3 ± 3.0	
PR6_041	0.02	361	193	0.55	32.50 ± 0.54	0.0540 ± 0.0045	195.3 ± 3.2	
PR6_042	0.53	220	161	0.75	30.56 ± 0.68	0.0403 ± 0.0053	207.5 ± 4.5	
PR6_043	1.49	466	272	0.60	33.06 ± 0.53	0.0515 ± 0.0047	192.1 ± 3.0	
PR6_044	0.56	771	426	0.57	35.58 ± 0.44	0.0497 ± 0.0032	178.7 ± 2.2	
PR6_045	0.00	408	219	0.55	36.09 ± 0.59	0.0612 ± 0.0028	176.2 ± 2.8	discordant
PR6_046	0.01	618	337	0.56	34.43 ± 0.51	0.0474 ± 0.0033	184.6 ± 2.7	
PR6_047	0.83	967	749	0.79	51.62 ± 0.78	0.0484 ± 0.0041	123.7 ± 1.9	
PR6_048	1.15	421	218	0.53	55.04 ± 0.91	0.0421 ± 0.0052	116.1 ± 1.9	
PR6_049	1.63	579	371	0.66	33.77 ± 0.49	0.0480 ± 0.0041	188.1 ± 2.7	
PR6_050	2.26	267	141	0.54	33.87 ± 0.64	0.0457 ± 0.0056	187.5 ± 3.5	
PR6_051	0.00	677	376	0.57	27.08 ± 0.28	0.0595 ± 0.0016	233.8 ± 2.4	discordant
PR6_052	2.83	162	120	0.76	29.96 ± 0.66	0.0412 ± 0.0083	211.7 ± 4.6	
PR6_053	1.41	561	185	0.34	29.72 ± 0.31	0.0511 ± 0.0031	213.3 ± 2.2	
PR6_054	0.19	513	396	0.79	38.12 ± 0.56	0.0487 ± 0.0045	166.9 ± 2.4	
PR6_055	0.43	390	266	0.70	33.11 ± 0.58	0.0557 ± 0.0041	191.8 ± 3.3	
PR6_056	0.00	449	172	0.39	33.72 ± 0.46	0.0552 ± 0.0023	188.4 ± 2.6	discordant
PR6_057	0.00	631	453	0.74	46.77 ± 0.66	0.0471 ± 0.0020	136.4 ± 1.9	
PR6_058	0.00	567	230	0.42	33.66 ± 0.47	0.0481 ± 0.0016	188.7 ± 2.6	
PR6_059	0.00	873	314	0.37	32.81 ± 0.40	0.0508 ± 0.0016	193.5 ± 2.3	
PR6_060	0.00	255	145	0.58	56.91 ± 1.35	0.0470 ± 0.0033	112.3 ± 2.6	
PR6_061	0.77	209	161	0.79	20.76 ± 0.31	0.0453 ± 0.0049	303.2 ± 4.4	
PR6_062	4.47	137	50	0.37	32.50 ± 0.84	0.0597 ± 0.0095	195.3 ± 5.0	
PR6_063	0.89	933	292	0.32	34.12 ± 0.38	0.0486 ± 0.0023	186.2 ± 2.1	
PR6_064	0.36	132	73	0.56	32.21 ± 0.83	0.0586 ± 0.0067	197.1 ± 5.0	
PR6_065	0.92	195	99	0.52	56.99 ± 1.36	0.0479 ± 0.0071	112.1 ± 2.6	
PR6_066	1.73	872	1018	1.20	24.31 ± 0.26	0.0598 ± 0.0038	259.9 ± 2.8	discordant
PR6_067	0.02	466	163	0.36	34.81 ± 0.50	0.0459 ± 0.0029	182.6 ± 2.6	
PR6_068	3.19	487	379	0.80	25.36 ± 0.46	0.0799 ± 0.0069	249.4 ± 4.4	discordant
PR6_069	2.12	280	168	0.62	34.84 ± 0.61	0.0465 ± 0.0061	182.4 ± 3.1	
PR6_070	2.08	624	320	0.53	31.53 ± 0.50	0.0488 ± 0.0051	201.3 ± 3.1	
PR6_071	0.00	226	103	0.47	35.33 ± 0.70	0.0513 ± 0.0024	179.9 ± 3.5	
PR6_072	0.73	259	77	0.30	31.32 ± 0.58	0.0504 ± 0.0040	202.6 ± 3.7	
PR6_073	0.08	419	175	0.43	57.19 ± 1.05	0.0518 ± 0.0046	111.8 ± 2.0	
PR6_074	0.00	408	186	0.47	35.22 ± 0.65	0.0653 ± 0.0033	180.5 ± 3.3	discordant
PR6_075	0.52	225	154	0.70	35.63 ± 0.70	0.0626 ± 0.0069	178.4 ± 3.5	
PR6_076	0.00	197	159	0.83	14.94 ± 0.21	0.0538 ± 0.0023	417.6 ± 5.6	
PR6_077	1.92	400	185	0.47	34.25 ± 0.59	0.0485 ± 0.0056	185.5 ± 3.1	
PR6_078	0.11	697	479	0.71	33.80 ± 0.40	0.0537 ± 0.0042	188.0 ± 2.2	
PR6_079	0.00	601	499	0.85	34.61 ± 0.50	0.0489 ± 0.0016	183.6 ± 2.6	
PR6_080	0.71	461	206	0.46	38.49 ± 0.64	0.0463 ± 0.0039	165.3 ± 2.7	
PR6_081	0.00	634	443	0.72	32.61 ± 0.42	0.0570 ± 0.0025	194.7 ± 2.5	discordant
PR6_082	0.00	820	335	0.42	35.76 ± 0.51	0.0506 ± 0.0016	177.8 ± 2.5	

Errors are 1-sigma; Pb_c and Pb^* indicate the common and radiogenic portions, respectively.

(1) Common Pb corrected by assuming $^{206}Pb/^{238}U$-$^{208}Pb/^{232}Th$ age-concordance

(2) The degree of discordance for an analyzed spot indicates the chronological difference between the two ages determined by Pb-Pb and U-Pb methods, and is defined as $\{1 - (^{238}U/^{206}Pb^*\ \text{age})/(^{207}Pb^*/^{206}Pb^*\ \text{age})\} \times 100$ (%) (e.g., Song *et al.*, 1996).

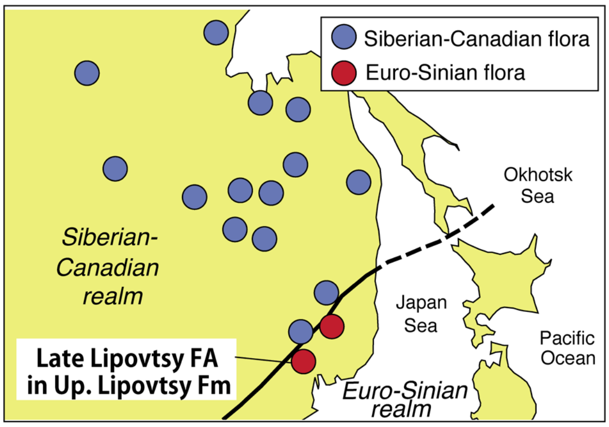

Fig. 5. Albian (late Early Cretaceous) paleofloristic biogeography in Far East Asia (simplified from Kirillova, 2018).
Note that the study section in southern Primorye occurs immediately on the south of the boundary between the Siberian-Canadian and Euro-Sinian floristic realms. The Late Lipovtsy FA, as well as the Tetori flora from Japan, likely represents one of the northern varieties in the Euro-Sinian floristic realm. Warm climate-adapted flora, together with the early angiosperms, gradually migrated toward high-latitude regions under the Early Cretaceous warming climate, and consequently reached southern Primorye by the Albian.

Albian (Fig. 2), the time lag between the Barremian in SW Japan and the Albian in Primorye was ca. 8 million years or more. This supports the latitude-relevant delay for the angiosperm appearance in the north in view of the claimed global warming during the Early Cretaceous in eastern Eurasia and the relevant gradual northward migration of angiosperms primarily from low-latitude regions (e.g. Axelrod, 1959; Brenner, 1976; Legrand *et al.*, 2021).

Provenance: The age spectrum of detrital zircons (Fig. 4C) clearly demonstrates that the main source of terrigenous clastics for the Albian Lipovtsy sandstone was Early Jurassic igneous rocks, with a minor contribution from Triassic and Middle Jurassic-Early Cretaceous ones. Late Paleozoic grains are present but lesser in amount, and Precambrian one is absent. This aspect is concordant with the basement geology of the L-G belt, in particular, the dominance in Early Jurassic zircons (over 60%) with subordinate Permo-Triassic ones likely reflecting the regional occurrence of the Jurassic granitoids in the L-G belt (Isozaki *et al.*, 2021). It is also noteworthy to recognize ca. 210–220 Ma (Norian, Triassic) zircon grains, as this age may possibly imply the derivation from the unique A-type granites recognized solely in the L-G belt and its extensions within Far East Asia (Isozaki *et al.*, 2023).

Although paleocurrent analyses have not been reported yet for the upper Lipovtsy Fm, the main terrigenous source is constrained by and large to the L-G belt. On the other hand, lesser input is suggested from the Khanka belt (GSC) and Nipponides elements on the east.

Comparison with neighboring basins in Far East: To examine the relative status of the Razdol'naya basin with respect to the overall Cretaceous sedimentary setting in Far East Asia, age spectra of detrital zircon are compared between the Lipovtsy sandstone and coeval Lower Cretaceous sandstones in the neighboring basins (Fig. 1B), i.e. the Dasanjiang basin in NE China/western Primorye and the Songliao basin in NE China.

The Dasanjiang basin occurs on the north of the Razdol'naya basin (Fig. 1B). According to the U-Pb ages of detrital zircons previously reported from the Albian Muling and Houshingou formations in NE China (Sun *et al.*, 2015; Zhang *et al.*, 2015), these sandstones are enriched in 190–160 Ma (Jurassic) zircons with minor amount of 500–400 Ma (early Paleozoic), 250 Ma (late Permian-early Triassic), and 110–100 Ma (Early Cretaceous) grains without Precambrian ones (Fig. 6B). They are thus essentially similar to that of the Razdol'naya basin (Fig. 6A), although the zircon flux from the typical Khanka basement rocks (500–400 Ma; Wilde *et al.*, 2010; Xu *et al.*, 2018) is more significant in the Dasanjiang sandstones. As to the underlying Barremian and Aptian sandstones, their age spectra are more or less the same as the Albian ones (Sun *et al.*, 2015; Zhang *et al.*, 2015). In short, all these Dasanjiang sandstones, deposited directly on the Jiamusi (GSC) basement rocks with 500-400 Ma and 250 Ma granitoids, likely received abundant clastics from them. The Early Jurassic grains, on the other hand, were likely derived from the Lesser Xing'an range in NE China of the west-neighboring L-G belt, as previously speculated (Sun *et al.*, 2015; Zhang *et al.*, 2015).

Nonetheless, a major difference exists in the extreme rareness of early Paleozoic grains in the Lipovtsy sandstone with respect to those of the Dasanjiang basin (Fig. 6A, B). This likely reflected the rock composition of the domestic provenance

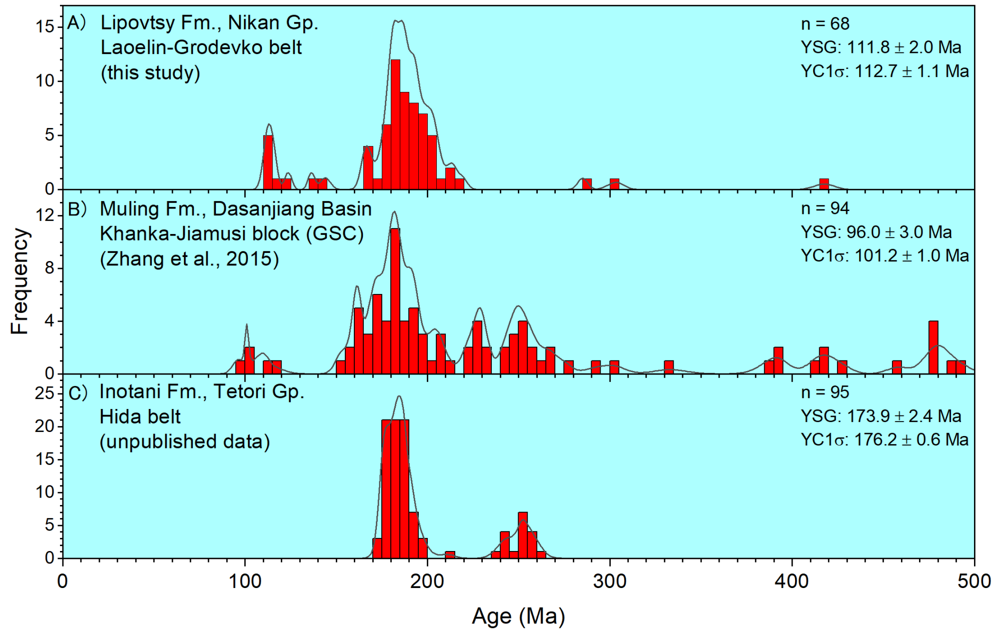

Fig. 6. Comparison of age spectra of detrital zircons among neighboring belts/units. A: Lipovtsy Fm (Nikan Gp) in L-G belt, Primorye (Sample PR6, this study), B: Muling Fm in Jiamusi block, NE China (Zhang *et al.*, 2015), C: Inotani Fm (Tetori Gp) in Hida belt, Japan (Isozaki *et al.*, in review).
Note that the late Early Cretaceous sandstone from the L-G belt (Primorye) share almost identical age spectra of detrital zircons not only with coeval sandstones in the neighboring basins on CAOB and GSC but also with the Tetori Gp on the Hida belt in Japan. This indicates that the sedimentary regime of relevant basins and provenance in Early Cretaceous Far East Asia was mostly monotonous before the major change after the late Albian.

for the Razdolʹnaya basin. As the basement of the Lipovtsy Fm in the L-G belt rarely contains early Paleozoic granitoids, if at all, its provenance was unique, whereas the Dasanjiang basin developed on the Jiamusi/Khanka blocks (GSC) naturally enriched with early Paleozoic granitoids.

The largest Late Jurassic to Cenozoic intracontinental sedimentary basin in Far East Asia is the Songliao basin in NE China (Fig. 1B). Some outcrop/drilled core samples of Cretaceous sandstones were analyzed by U-Pb dating of detrital zircons (Li *et al.*, 2012, 2020; Wang *et al.*, 2022). Their results clearly documented that all samples are dominated by the 270–250 Ma and 190–170 Ma zircons (spread sheet of analyzed zircon ages were not published, thus cannot be compared in Fig. 6). Nonetheless, their analyzed sandstones can be classified into 2 groups; i.e., one group without Precambrian grains and the other with many of them. The former are all Albian and older sandstones, whereas the latter are late Albian and younger sandstones, which are clearly separated stratigraphically by a remarkable mid-Cretaceous unconformity (Li *et al.*, 2020). The age spectra of the former group are essentially similar to the coeval sandstones of the Razdolʹnaya and Dasanjiang basins (Fig. 6A, B). The significant mid-Cretaceous unconformity likely suggests a major change in provenance-basin system, possibly due to a large-scale tectonic episode relevant to a new terrigenous flux with abundant Late Archean and Proterozoic zircons probably from North China block (Li *et al.*, 2012, 2020; Wang *et al.*, 2022).

The above comparison, in short, suggests two issues. First, at least from the Barremian to early Albian, the Razdolʹnaya basin was fed from the same provenance as the Dasanjiang and Songliao basins, which was most likely the domain characterized by the peculiar two granitoid ages; i.e., the L-G belt, but unlikely the Khanka/Jiamusi blocks (GSC). This suggests the mass production of terrigenous clastics occurred mostly on the eastern side of CAOB, and also the associated extensive coverage of thick sedimentary drapes over the conterminous Far East Asia during most of the Early Cretaceous.

Connection to the Hida belt: On the opposite coast of the Japan Sea, the Hida belt in central Japan is recently correlated with the L-G belt in the conterminous eastern Eurasia on the basis of their basement granitoid assemblages (Fig. 7; Isozaki *et al.*, 2021, 2023). Judging from the non-marine litho-

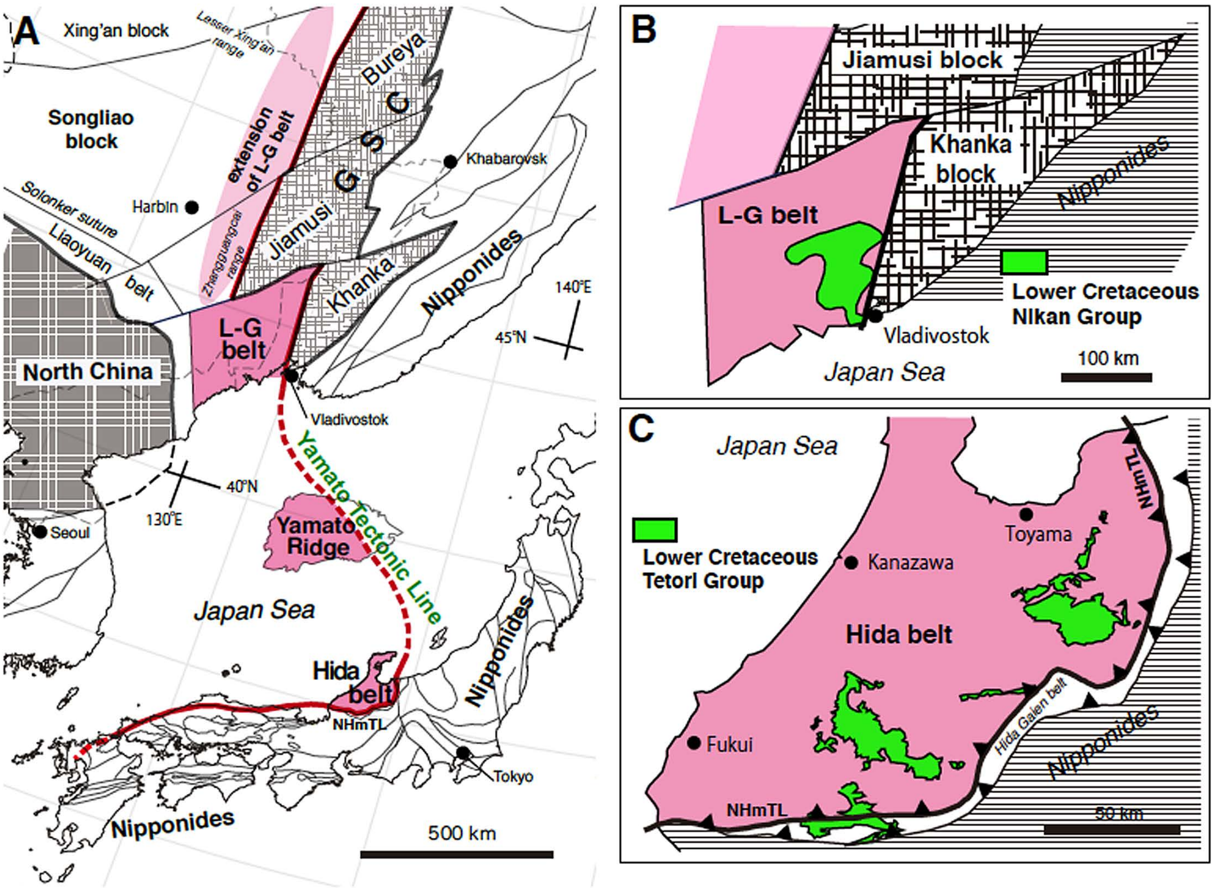

Fig. 7. Geotectonic framework of Far East Asia (A; modified from Isozaki *et al.*, 2023) and distribution of Lower Cretaceous non-marine strata in the Laoelin-Grodekov belt, Primorye (B: the Nikan Group; Krillova, 2018) and that in the Hida belt, central Japan (C: the Tetori Group; Matsukawa *et al.*, 2014).
Note that the Lipovtsy Fm, as well as the Tetori Gp, was deposited on the L-G belt between the CAOB and GSC-Nipponides, which was located close to the border between the Siberian-Canadian and Euro-Sinian floristic realms.

facies and plant fossils, the Lower Cretaceous Tetori Gp in the Hida belt has been correlated with the Lower Cretaceous strata in Primorye, including the Nikan Gp analyzed in this study. Figure 6C shows the age spectrum of detrital zircons in one of the sandstones (the Inotani Fm) of the Tetori Gp (Isozaki *et al.*, in review), which appears similar to that of the Lipovtsy sandstone (Fig. 6A). In particular, the most striking affinity exists in the dominance of Early Jurassic grains with minor amounts of Permo-Triassic ones, which is in good accordance with the basement geology of both belts.

These Lower Cretaceous sandstones of the Tetori and Nikan groups share almost the same age spectrum with those from the Dasanjian and Songliao basins in the continental interior (Fig. 6), suggesting the regional development of a sedimentary system with rather monotonous terrigenous sources/depositional sites throughout the Early Cretaceous Far East Asia. Nonetheless, there are some differences among these basins as to the presence/absence of Early Cretaceous, early-middle Paleozoic, or Precambrian grains (Fig. 6). In addition to the overall uniform sources, some local geological uniqueness may be stigmatized in detrital signature for each area. Details on local provenance for the Tetori basin will be discussed elsewhere.

It is also worth noting that the Cretaceous shallow marine sandstones in SW and NE Japan (e.g. Nakahata *et al.* 2016; Tsutsumi *et al.*, 2018; Hasegawa *et al.*, 2020; Ishizaka *et al.*, 2021) show slightly different age spectra of detrital zircons with respect to the above-discussed mid-continent sandstones, particularly in the absence of Precambrian-Paleozoic and early Mesozoic grains in the Upper Cretaceous sandstones. This may imply the development of a distinct provenance for the Cretaceous depositional system for Nipponides on the Pacific-side of GSC, which will be discussed more in detail elsewhere.

Conclusions

The present study on U-Pb dating of detrital zircons for a Lower Cretaceous sandstone (Upper Lipovtsy Fm) in the Laoelin-Grodekov (L-G) belt, SW Primorye, confirmed the depositional age of the analyzed sandstone at the Albian or younger, and revealed the following new aspects of the Lower Cretaceous non-marine sedimentary system in Far East Asia and associated flora.

1. The Albian sandstone of the L-G belt in southern Primorye shares almost the same age spectrum as coeval sandstones deposited in the neighboring Dasanjiang basin of the Jiamusi block (=GSC) on the north, Songliao basin of the CAOB on the west, and also the Tetori basin of the Hida belt (=L-G belt) on the south. This suggests the development of a relatively monotonous non-marine provenance-basin system in the continental interior of Early Cretaceous Far East Asia.
2. The emergence timing of angiosperms in Primorye, recorded in the Late Lipovtsy FA, is for the first time constrained to no earlier than the Albian, which is significantly later than in SW Japan, suggesting the northward migration of angiosperms along time during the late Early Cretaceous global warming.
3. The similarities, not only in ages of detrital grains but also in floristic characteristics, of the Lower Cretaceous sandstones altogether support the pre-Japan Sea geotectonic connection between the L-G belt in Russia/China/N. Korea and the Hida belt in central Japan, via the Yamato Ridge prior to the Miocene opening of the Japan Sea.

Acknowledgements

Dr. Atsushi Yabe provided many valuable comments on the Early Cretaceous plant paleobiogeography in Far East Asia. Constructive review comments from Dr. Ken'ichiro Tani improved the original MS. Tomoyo Tobita and Yuto Ishizaka helped in sample collection in Primorye. This research was supported by Kakenhi (no. 19H00711 to YI) from Ministry of Education, Culture and Sports, Japan, and by the Russian Foundation for Basic Research (Grant no. 19-05-00229 to VN).

References

Ando, H. and Takahashi, M. (2017) Reconstruction of the Cretaceous Paleo-Japan continental arc-trench system reconsidered from Cretaceous geologic records in the Japanese Islands. *Fossils*, **102**: 43–62. (in Japanese with English abstract)

Axelrod, D.I. (1959) Polarward migration of early angiosperm flora. *Science*, **130**: 203–207.

Brenner, G.J. (1976) Middle Cretaceous floral provinces and early migration of angiosperms In Beck, C.B. ed. Origin and early evolution of angiosperms, Columbia Univ. Press, pp. 23–47, New York.

Brenner, G.J. (1996) Evidence for the earliest stage of angiosperm pollen evolution: a paleoequatorial section from Israel. In Tayler, D. and Hickey, L.J. eds. Flowering plant origin, evolution, and phylogeny. Chapman & Hall, pp. 91–115, New York.

Cohen, K.M., Finney, S.C., Gibbard, P.L. and Fan, J.-X. (2013): The ICS International Chronostratigraphic Chart. *Episodes*, **36**: 199–204. https://stratigraphy.org/chart (updated in 2023)

Dickinson, W.R. and Gehrels, G.E. (2009) Use of U-Pb ages of detrital zircons to infer maximum depositional ages of strata: A test against a Colorado Plateau Mesozoic database. *Earth and Planetary Science Letters*, **288**: 115–125.

Domier, M. (2018) Early Paleozoic tectonics of Asia: towards a full-plate model. *Geoscience Frontiers*, **9**: 789–862, https://doi.org/10.1016/j.gsf.2017.11.012

Golozoubov, V.V., Markevich, V.S. and Bugdaeva, E.V. (1999) Early Cretaceous changes of vegetation and environment in East Asia. *Palaeogeography*, *Palaeoclimatology*, *Palaeoecology*, **153**: 139–146.

Hasegawa, R., Isozaki, Y., Yamamoto, A. and Tsutsumi, Y. (2020) Secular change in fore-arc sandstones and their provenance in Cretaceous Southwest Japan: U-Pb dating of detrital zircons. *Journal of Geography*, **129**: 397–421. doi:10.5026/jgeography.129.397. (in Japanese with English abstract)

Hoffman, P.F. (1991) Did the breakout of Laurentia turn Gondwanaland inside out? *Science*, **252**: 1409–1412, https://doi.org/10.1126/science.252.5011.1409

Ishizaka, Y., Isozaki, Y. and Tsutsumi, Y. (2021): Provenance change in Cretaceous-Paleogene forearc in Western Hokkaido: U-Pb dating of detrital zircons from the Yezo Group. *Journal of Geography* (*Chigaku Zasshi)*, **130**, 63–83. doi:10.5026/jgeography.130.63(in Japanese with English abstract)

Isozaki, Y. (2019) A visage of Paleozoic Japan: geotectonic and paleobiogeographical significances of Greater South China. *Island Arc*, **28**: e12296. https://doi.org/10.1111/iar.12296.

Isozaki, Y., Aoki, K., Sakata, S. and Hirata, T. (2014) The eastern extension of Paleozoic South China in NE Japan evidenced by detrital zircon U-Pb ages. *GFF*, **136**: 116–119. http://dx.doi.org/10.1080/11035897.2014.893254

Isozaki, Y., Hasegawa, R., Nakano, T., Tsutsumi, Y., Nechaev, V., Zakharov, Y. and Popov, A. (2021). Zircon U-Pb ages of Permian-Triassic granitoids in the southeastern Laoelin-Grodekov belt, Primorye, Far East Russia: possible correlation with the Hida belt in central Japan. *Bulletin of National Museum of Nature and Science, Tokyo.* Ser. C, **47**: 25–39. doi:10.50826/bnmnsgeopaleo.47.0_25.

Isozaki, Y., Nakahata, H., Zakharov, Y., Popov, A., Sakata, S. and Hirata, T. (2017). Greater South China extended to the Khanka block: detrital zircon geochronology of middle-upper Paleozoic sandstones in Primorye, Far East Russia. *Journal of Asian Earth Sciences,* **108**: 136–149. http://dx.doi.org/10.1016/j.jseaes.2017.06.027

Isozaki, Y., Sawaki, Y., Iwano, H., Hirata, T. and Kunugiza, K. (2023) Late Triassic A-type granite boulders in Lower Cretaceous conglomerate of the Hida belt, Japan: origin and bearing on the Yamato Tectonic Line in Far East Asia. *Island Arc*, **32**: e12475. https://doi.org/10.1111/iar.12475

Jahn, B.M. (2004). The Central Asian Orogenic Belt and growth of the continental crust in the Phanerozoic. in Malpas, J., Fletcher, C.J.N., Ali, J.R. and Aitchison, J.C. eds., Aspects of the tectonic evolution of China. *Geological Society of London Spec. Publ*., **226**: 73–100.

Kemkin, I.V. (2012) Tectono-stratigraphy as a reflection of accretion tectonics processes (on an example of the Nadankhada-Bikin Terrane of the Sikhote-Alin Jurassic accretionary prism, Russia Far East). In Elitok, O. (ed.) Stratigraphic analysis of layered deposits, InTech, Vladivostok, pp. 279–298.

Khanchuk, A.I., Ratkin, V.V. and Ryazantoseva, M.D. (1996) Geology and mineral deposits of Prymorsky Krai. Dalʹnauka, Vladivostok, 56 pp.

Kimura, T. (1979) Late Mesozoic paleofloristic provinces in East Asia. *Proceeding of Japan Academy*, **55B**: 425–430.

Kirillova, G.L. (2018) Cretaceous tectonic and biotic evolution of the southeastern Russian continental margin. *Island Arc*, **27**: e12238. https://doi.org/10.1111/iar.12238

Krassilov, V.A. (1967) The Early Cretaceous flora of the southern Primorye and its significance for the stratigraphy. Nauka, Moscow 264, 93p. (in Russian)

Kojima, S., Kemkin, I.V., Kametaka, M. and Ando, A. (2000) A correlation of accretionary complexes of southern Sikhote Alin of Russia and the Inner zone of southwest Japan. *Geoscience Journal*, **4**: 175–185.

Kosenko, I.N., Sha, J.G. and Shurygin, B.N. (2021) Upper Mesozoic stratigraphy of Sikhote-Alin (Russian Far East) and northeastern China: non-marine and marine correlatiobs Part 2: Barremian-Albian. *Cretaceous Research*, **124**: 10812. https://doi.org/10.1016/j.cretres.2021.104812.

Kovaleva, T.A., Markevich, V.S., Bugdaeva, E.V., Volynets, E. B. and Afonin, M.A. (2016) New data on palynostratigraphy of the Lipovtsy Formation in the Razdolʹnaya coal basin (southern Primorye). *Russian Journal of Pacific Geology*, **10**: 50–62. doi: 10.1134/S1819714016010061.

Legrand, J., Yamada, T. and Nishida, H. (2014) Palynofloras from the Upper Barremian–Aptian Nishihiro Formation (Outer zone of southwest Japan) and the appearance of angiosperms in Japan. *Journal of Plant Research*, **127**: 221–232. doi: 10.1007/s10265-013-0619-6.

Legrand, J., Terada, K., Yukawa, H. and Nishida, H. (2019) Report of *Clavatipollenites hugheshii* from the Kitadani Formation: first angiosperm record from the Lower Cretaceous of Inner Japan. *Memoir Fukui Pref. Dinosaur Mus.*, **18**: 21–31.

Legrand, J. Yamada, T., Terada, K. and Nishida, H. (2021) Palynofloras from the Itsuki and Kuwajima formations of the Tetori Group and their correlation with paleofloristic provinces of eastern Asia. *Paleontological Research*, **25**: 177–190. https://doi.org/10.2517/2020 PR017.

Li, S.Q., Chen, F.K., Siebel, W., Wu, J.D., Zhu, X.Y., Shan, X.L. and Sun, X.M. (2012) Late Mesozoic tectonic evolution of the Songliao basin, NE China: evidence from detrital zircon ages and Sr-Nd isotopes. *Gondwana Research*, **22**: 943–955.

Li, S.Q., He, S. and Chen, F.K. (2020) Provenance change across the mid-Cretaceous unconformity in basins of northeastern China: evidence for an integrated paleolake subsystem and tectonic transformation. *Geol. Soc. Amer. Bull.*, **132**: 185–198. https://doi.org/10.1130/B35660.1.

Maruyama, S., Liou, J.G. and Seno, T. (1989) Mesozoic and Cenozoic evolution of Asia. In Ben-Avraham, Z. (Ed.), The Evolution of the Pacific Ocean Margins, 75–99. Oxford Univ. Press, New York.

Matsukawa, M., Fukui, M., Ogawa, Y., Tago, T., Koarai, K., Ohira, H. and Hayashi, K. (2014) Stratigraphy of the Tetori Group and Jinzu Group (new name) in Gifu and Toyama prefectures, Central Japan. *Journal Geological Society of Japan*, **120**: 147–164. (in Japanese with English abstract). https://doi.org/10.5575/geosoc.116.S83

Melʹnikov, N.G. and Izosov, L.A. (1984) Structure-formation zoning of Primorye. *Tikhookeanskaya Geologiya*, **1**: 53–61 (in Russian).

Nakahata, H., Isozaki, Y., Tsutsumi, Y. and Iwamoto, N. (2016a): Age spectra of detrital zircons from shallow marine Cretaceous in southern Kanto, SW Japan: Change in composition of fore-arc sandstones in response to the rejuvenation of provenance crust. *Journal of Geography* (*Chigaku Zasshi)*, **125**, 353–380. doi:10.5026/jgeography.125.353 (in Japanese with English abstract)

Ohana, T. and Kimura, T. (1995) Late Mesozoic phytogeography in eastern Eurasia, with special reference to the origin of angiosperms in time and site. Proc. 15th Int. Symp. Kyungpook National Univ.: 293–328.

Otofuji, Y. and Matsuda, T. (1987) Amount of clock-wise rotation of Southwest Japan-fan shaped opening of the southwestern part of the Japan Sea. *Earth and Planetary Science Letters*, **85**: 289–301.

Sengör, A.M.C. and Natalʹin, B.A. (1996) Plate tectonics of Asia: fragments of a synthesis. In Yin, A. and Harrison, M. (Eds.), The Tectonic Evolution of Asia, Rubey Colloquim, Cambridge Univ. Press, pp. 486–640.

Stacey, J.S. and Kramers, J.D. (1975) Approximation of terrestrial lead isotope evolution by a two-stage model. *Earth and Planetary Science Letters*, **26**: 207–221.

Sun, M.D., Chen, H.L., Zhang, F.Q., Wilde, S.A., Minna, A., Lin, X.B. and Yang, S.F. (2015) Cretaceous provenance change in the Hegan Basin and its connection with the Songliao Basin, NE China: evidence for lithospheric extension driven by paleo-Pacific roll-back. In Gibson, G.M., Roure, F. and Manatschal, G. (Eds.), Sedimentary basins and crustal processes at continental margins: from modern hyper-extended margins to deformed ancient analogues. *Geol. Soc. London*, *Spec. Publ*., **413**: 91–117.

Tamaki, K. (1988) Geological structure of the Japan Sea and its tectonic implications. *Bulletin of the Geological Survey of Japan*, **39**: 269–365.

Tanaka, K (1977) Chapter 15 Cretaceous System. In Tanaka, K. and Nozawa, T. (Eds.), Geology and Mineral Resources of Japan, pp. 182–206, Geological Survey Japan, Kawasaki.

Tsutsumi, Y., Horie, K., Sano, T., Miyawaki, R., Momma, K., Matsubara, S., Shigeoka, M. and Yokoyama, K. (2012) LA-ICP-MS and SHRIMP ages of zircons in chevkinite and monazite tuffs from the Boso Peninsula, Central Japan. *Bulletin of the National Museum of Nature and Science*, *Series C,* **38**: 15–32.

Tsutsumi, Y., Isozaki, Y., Kani, T. and Nakahata, H. (2018): Detrital zircon U-Pb dating of Cretaceous sandstones from Amakusa-Mifune district, central Kyushu, Japan: Provenance and transition of fore-arc clastic rocks in Cretaceous Japan. *Journal of Geography* (*Chigaku Zasshi)*, **127**, 21–51 doi:10.5026/jgeography.127.21 (in Japanese with English abstract)

Tunheng, A. and Hirata, T. (2004) Development of signal smoothing device for precise elemental analysis using laser ablation-ICP-mass spectrometry. *Journal of Analytical Atomic Spectrometry*, **7**: 932–934.

Vakhraneev, V.A. (1978) The climate of the Northern Hemisphere in the Cretaceous in the light of paleobotanical data. *Paleontological Journal*, **12**: 143–154.

Volynets, E. and Bugdaeva, E. (2017) The Aptian-Cenomanian flora of the Razdolnaya coal basin (Primorye region, Russia). *Island Arc*, **26**: e12171. https://doi.org/10.1111/iar.12171

Volynets, E.B. and Malinovsky, A.I. (2020) Coal-bearing deposits and floras of Ilyichevka coal field in Razdolnensky basin of Primorye. Abst. Materials of the 10th All-Russia Meeting (Cretaceous system of Russia and neighboring countries: problems of stratigraphy and paleogeography, Magadan, September 20–25, 2020): 50–52. (in Russian)

Wang, S.Y., Cheng, Y.H., Jin, R.S., Miao, P.S., Zhang, T.F., Xu, Z.L., Ao, C., Teng, X.M. and Cheng, X.Y., (2022) Detrital zircon U-Pb ages of the Cretaceous strata in the southern Songliao basin, NE China: constraints on basin-and-range evolution. *Sedimentary Geology*, **433**: 106133.

Wilde, S.A., Wu, F.Y. and Zhao, G.C. (2010) The Khanka Block, NE China, and its significance for the evolution of the Central Asian Orogenic Belt and continental accretion: *Geological Society*, *London*, *Special Publications*, **338**: 117–137. doi:10.1144/SP338.6.

Xu, T., Xu, W.L., Wang, F., Ge, W.C. and Sorokin, A.A. (2018) Geochronology and geochemistry of early Paleozoic intrusive rocks from the Khanka Massif in the Russian Far East: Petrogenesis and tectonic implications. *Lithos*, **300–301**: 105–120. doi:10.1016/j.lithos.2017.12.004.

Yabe, A., Terada, K. and Sekido, S. (2003) The Tetori-type Flora, revisited: a review. *Memoir Fukui Prefectural Dinosaur Museum*, **2**: 23–42.

Zakharov, Y.D., Panchenko, I.V. and Khanchuk, A.I. (1992) A field guide to the Late Paleozoic and Early Mesozoic circum-Pacific bio- and geological events. FEGI FEB RAS, Vladivostok, 88pp.

Zhang, F.Q., Chen, H.L., Batt, G.E., Dilek, Y., A, M.N, Sun, M.D., Yang, S.F. and Zhao, X.Q (2015) Detrital zircon U-Pb geochronology and stratigraphy of the Cretaceous Sanjiang basin in NE China: provenance record of an abrupt tectonic switch in the mode of and nature of the NE Asian continental margin evolution. *Tecotonophysics*, **665**: 58–78.